Arthritis Research & Therapy

RESEARCH

Open Access

Chondrocyte lysates activate NLRP3 inflammasome-induced pyroptosis in synovial fibroblasts to exacerbate knee synovitis by downregulating caveolin-1

Xue Du[1,3,4†], Ruonan Liu[1,4†], Zongrui Jiang[1,4], Chengyun Zhang[1,4], Zhijian Yang[1,4], Shu Hu[2,5,6,7*] and Zhiqi Zhang[1,4*]

Abstract

Background Synovitis, among the most common signs of early-stage osteoarthritis (OA), is mainly mediated by fibroblast-like synoviocytes (FLSs). Cartilage destruction creates chondrocyte lysates (CLs) that activate synovial inflammation. A comprehensive understanding of chondrocyte–FLS communication might offer novel, specific therapeutic targets for treating synovitis and OA. Hence, we sought to uncover the specific role of CLs in OA-FLSs and synovitis.

Methods Isolated CLs were cocultured with FLSs to test whether they could stimulate synovial inflammation. A model of medial meniscus destabilization was prepared in C57BL/6 mice and NLRP3 knockout mice, and adeno-associated virus overexpressing Caveolin-1 (CAV1) was intra-articularly injected for 8 weeks once a week after dissection of the medial meniscus (DMM). Proteins expressed in FLSs with and without CL coculture were screened using liquid chromatography-tandem mass spectrometry to identify CL-specific regulators of NLRP3 inflammasome-mediated pyroptosis.

Results CLs were engulfed by FLSs, which aggravated inflammatory cytokine release and NLRP3 inflammasome-mediated FLS pyroptosis. NLRP3 expression was significantly upregulated in human OA-FLSs and FLSs cocultured with CLs, while CAV1 was downregulated. CAV1 overexpression reversed the inflammatory phenotype in FLSs and simultaneously rescued pyroptosis in CL-pre-treated FLSs. Both synovial hyperplasia and inflammatory infiltration in C57BL/6 mice with DMM surgery were alleviated after intra-articular AAV-CAV1 injection. Moreover, the CL-specific protein LIM-containing lipoma preferred partner (LPP) markedly exacerbated FLS pyroptosis and inflammation.

Conclusions CLs were endocytosed by FLSs through CAV1, and the CL-specific protein LPP stimulated NLRP3 inflammasome-mediated pyroptosis and synovitis by inhibiting CAV1 expression. Our findings offer a novel therapeutic target for treating synovitis.

†Xue Du and Ruonan Liu contributed equally to this work.

*Correspondence:
Shu Hu
hushusysu@163.com
Zhiqi Zhang
zhzhiqi@mail.sysu.edu.cn

Full list of author information is available at the end of the article

Keywords Caveolin-1, Chondrocyte lysate, Fibroblast-like synoviocyte, LIM-containing lipoma preferred partner, NLRP3

Introduction

Osteoarthritis (OA) is one of the most common ageing and posttraumatic degenerative diseases and causes pain, stiffness, deformity and eventual disability. Studies have shown that over 22% of adults older than 40 years have OA of the knee, and it is estimated that over 500 million individuals are currently affected by OA worldwide [1]. In recent years, OA has no longer been viewed as a degenerative disease but rather as low-grade inflammation that is driven in part by the innate immune system. Innate immune cells recognise damage-associated molecular patterns (DAMPs) to produce inflammatory mediators and trigger inflammation [2]. In OA, the main source of DAMPs is cartilage matrix breakdown products, which are released into the synovial cavity and stimulate the innate immune system in the synovium [3]. Synovitis often precedes OA and is considered a sign of early OA. Therefore, to cure OA at an early stage, elucidating the mechanism of low-grade inflammation in OA is important.

In addition to several immune cells, such as macrophages, fibroblast-like synoviocytes (FLSs) are among the predominant cell types in the synovium. Aberrant hyperproliferation of FLSs results in synovial hyperplasia, a common feature of synovitis. Hence, to cure synovitis at an early stage, it is necessary to modulate the cellular homeostasis of FLSs. FLSs secrete several inflammatory mediators into the synovial fluid (SF). These mediators in the SF activate the expression and production of metalloproteinases in chondrocytes, which can lead to a vicious cycle [4]. As previously reported, DAMPs likely contribute to the pathological association of ageing with OA [5, 6]. DAMPs interact with pathogen-recognition receptors (PRRs), such as Toll-like receptors (TLRs) and Nod-like receptors (NLRs), and trigger the intracellular NLR family pyrin domain containing 3 (NLRP3) inflammasome [7]. Previous studies have suggested that NLRP1/3 inflammasome-activated pyroptosis in FLSs plays an important role in synovitis [8]. Upon activation, PRRs polymerise and then recruit apoptosis-associated speck-like protein containing a CARD (ASC) and caspase-1 to assemble into inflammasomes, which in turn activate caspase-1. Activated caspase-1 then cleaves precursors of the proinflammatory cytokines IL-1β and IL-18 to promote their maturation and release; furthermore, activated caspase-1 cleaves gasdermin D (GSDMD) to release its active N-terminal fragment. This N-terminal fragment of GSDMD perforates the cell membrane and triggers lytic cell death, which is also known as pyroptosis [9–12]. In vivo knockdown of NLRP3 was shown to alleviate synovitis and the OA phenotype in mice [13]. Although NLRP3 is considered an essential regulator of synovitis, the specific mechanism upstream of NLRP3 activation in the OA synovium needs to be verified.

Recent studies have reported that novel chondrocyte lysates (CLs) are associated with OA development [14–16]. Cartilage injury and degeneration lyse chondrocytes to form CLs that drift in the SF. Stimulation of either primary human synoviocytes or chondrocytes with soluble fractions of the lysates resulted in significantly elevated levels of expression of multiple genes encoding inflammatory and degradative mediators [14]. These specific CLs induce NLRP3 inflammasome activation in joints and may contribute to OA. However, relatively few studies have reported the effects of CLs on the NLRP3 inflammasome in FLSs. Moreover, NLPR3 is a cytosolic receptor, and understanding how CLs activate a receptor in the cytoplasm is important. One of the most important biological processes by which individual cells absorb macromolecules or particles is endocytosis. Among several molecules on the cell membrane that regulate endocytosis is caveolin-1 (CAV1), an important scaffold protein on the caveolae plasma membrane. It specifically binds several signalling molecules through its scaffolding domain and plays a vital role in lipid metabolism [17], cholesterol transport [18], and signal transduction [19]. Many studies have shown that caveolin-1 is involved in the caveolae-mediated transcytosis pathway, which is also currently exploited to deliver biological macromolecules and functionalized nanoparticles [20, 21]. The CAV1 gene is involved in cellular activities, as it regulates various signalling pathways (such as the PINK-1/Parkin, ERK and MAPK pathways) [22–24]. The transcription of CAV1 is also involved in the proinflammatory effect of DAMPs after tissue injury [25], and CAV1 may also act as an upstream protein that regulates NLRP3-mediated pyroptosis [26, 27]. CAV1 also contributes to the pathogenesis of OA by mediating chondrocyte senescence. Treatment of articular chondrocytes with IL-1β and hydrogen peroxide upregulated the expression of CAV1 and induced cellular senescence. Downregulation of CAV1 expression with antisense oligonucleotides prevented chondrocyte senescence induced by these stimuli [28]. Therefore, we hypothesise that CAV1 may play a role in regulating the phagocytosis of DAMPs by FLSs and stimulating the NLRP3 inflammasome to promote synovitis in OA.

In this study, we demonstrated the important role of CLs in the inflammatory phenotype of FLSs and synovitis, which are consumed by FLSs through endocytosis

regulated by CAV1. Further studies indicated that CLs suppressed the expression of CAV1, resulting in NLRP3 inflammasome activation in FLSs in vitro. In vivo overexpression of CAV1 alleviated synovitis in a DMM-induced OA model. There are literature reports that the expression level of LIM-containing lipoma preferred partner (LPP) can represent the grading changes of OA at different stages and degrees of synovitis, as well as its interaction at sites of focal adhesion in OAFLS [29]. Moreover, LPP was identified as a CL-specific protein that activates the NLRP3 inflammasome in FLSs. Thus, our study offers potential therapeutic targets for synovitis treatment.

Materials and methods

FLS isolation and cell culture

OA-FLSs were isolated from OA patients ($n = 10$) who underwent total knee arthroplasty (TKA) at the First Affiliated Hospital of Sun Yat-sen University. Corresponding control FLSs were harvested from patients who underwent arthroscopy with meniscus injury or anterior cruciate ligament tear (ACLT) ($n = 10$) and who displayed no synovitis, cartilage injury or degeneration (Table S1). The synovium was then digested overnight with 2 mg/ml type I collagenase (Sigma). The cell supernatant was filtered at 0.70 μm and cultured in Dulbecco's modified Eagle's medium (DMEM) supplemented with 10% foetal bovine serum (FBS) under 5% CO_2 at 37 °C. FLSs were then detached with 0.25% trypsin-EDTA after they reached 70–80% confluency and added to new medium.

Chondrocyte cell lysate isolation

Cartilage was also harvested from OA patients undergoing TKA and digested overnight by collagenase P (Roche). The chondrocytes were cultivated and passaged to P1–P4. The chondrocytes were then detached with 0.25% trypsin-EDTA, frozen (-80 °C or dry ice) and thawed (4 °C) 4 times, and centrifuged at 4 °C at 12,000 rpm for 10 min. The supernatants were acquired as CLs.

RNA extraction, reverse transcription, and qRT–PCR

Total RNA was extracted with TRIzol reagent, and reverse transcription was performed by using EVO M-MLV RTase according to the manufacturer's protocols. After reverse transcription, qRT–PCR was performed via 2× SYBR Green Pro Taq HS premix according to the manufacturer's instructions. The expression of each gene was calculated via normalization to the expression level of the housekeeping gene GAPDH. The primers used are listed in Table S2.

Western blot analysis

Total protein was extracted with radioimmunoprecipitation assay (RIPA) buffer, and SDS–PAGE was used to separate the proteins. After SDS–PAGE, we transferred the proteins to Immobilon-P membranes (0.45 or 0.22 *μm* pore size; Millipore, Billerica, MA, USA). The membranes were then blocked with skim milk and further incubated with primary antibodies overnight at 4 °C. After being rinsed with TBST, the membranes were incubated with an HRP-conjugated secondary antibody at room temperature for 1 h. The protein bands were visualised and detected with a chemiluminescence imaging system (Bio-Rad). ImageJ software was used to quantify the intensity of the bands. The antibodies used were as follows: *GAPDH* (1:1000 dilution, Proteintech), *NLRP3* (1:1000 dilution, AdipoGen), *caspase-1* (1:1000 dilution, AdipoGen), *GSDMD* (1:1000 dilution, CST), *IL-1β* (1:1000 dilution, CST), *IL-18* (1:1000 dilution, CST), *TLR4* (1:1000 dilution, Abcam), *caveolin-1* (1:1000 dilution, Abcam), *ERK* (1:2000 dilution, CST), *p-ERK* (1:1000 dilution, CST), *vimentin* (1:1000 dilution, CST), and *horseradish peroxidase (HRP)-conjugated secondary antibodies* (1:3000 dilution, CST).

Flow cytometry

Flow cytometry was used to evaluate the pyroptosis rates of the FLSs with an Annexin V-FITC/PI Apoptosis Detection Kit (MA0220). Specifically, the synoviocytes were detached, washed with PBS and stained with 5 μl of Annexin V-FITC and 10 μl of PI. The cells that were positive for Annexin V-FITC were considered pyroptotic cells. Cytoflex software was used to quantify the pyroptosis rate.

Immunofluorescence (IF) staining

The FLSs were fixed with 4% paraformaldehyde for 15 min and washed with PBS three times. The FLS nuclei were further permeated with PBS containing 0.3% Triton X-100 for 15 min. The cells were blocked with 5% BSA for 1 h and then incubated with the primary antibody overnight, after which they were incubated with secondary antibodies conjugated to goat anti-rabbit and anti-mouse immunoglobulin G (IgG) (Alexa Fluor 555, 488; CST). DAPI was used for nuclear staining. IF was observed via confocal microscopy. The primary antibodies used are listed in the Supplemental materials.

Cell proliferation assay

The cell culture conditions described above were also used for the cell proliferation assay. For the Cell Counting Kit-8 (CCK-8) assay, FLSs were seeded on 96-well plates at a density of 4000 cells per well. CLs were added after 24 h of incubation, and 10 *μl* of CCK-8 reagent (Beyotime, China) was added to each well after 48 h and incubated at 37 °C for 2 h. The absorbance at 450 nm was measured with a Varioskan LUX Multimode Microplate Reader (Thermo Fisher Scientific, MA, USA).

TUNEL staining

For the apoptosis assay, 1×10^6 cells/well were seeded in 6-well plates and cultured at 37 °C and 5% CO_2 in a humidified environment. The One Step TUNEL Apoptosis Assay Kit (Meilunbio) was used to detect apoptotic cells. Nuclei were stained with DAPI (blue). Fluorescence images were acquired with a fluorescence microscope (DMi8, Leica).

Enzyme-linked immunosorbent assay

The level of *IL-1β* in the supernatants of cultured cells following stimulation was detected via a Human IL-1β ELISA Kit (Neobioscience, China) according to the manufacturer's instructions. The absorbance at 450 nm was measured.

Transfection

siRNA against CAV1 and the corresponding negative control oligonucleotides were obtained from RiboBio (Guangzhou, China). When FLSs seeded into 6-well plates reached 70–80% confluence, they were transfected with these oligonucleotides via Lipofectamine 3000 (Lipo3000; Invitrogen, United States) following the manufacturer's protocol. The sequence used was as follows: siCAV1_001: CCACCTTCACTGTGACGAA.

Immunohistochemistry (IHC)

Paraffin-embedded sections were deparaffinised with xylene and boiled for antigen retrieval. Then, they were incubated with a hydrogen peroxide block for 10–15 min to reduce nonspecific background staining caused by endogenous peroxidase. The tissues were covered with CAV1 and vimentin or NLRP3 and vimentin primary antibodies (Abcam, 1:200) in working solutions and incubated overnight at 4 °C. The next day, the sections were incubated with an anti-rabbit or mouse IHC antibody (Abcam, USA) for 30 min at room temperature. The tissues were subsequently stained with haematoxylin and DAB. Finally, they were mounted with a cover glass and observed and photographed under a microscope.

Coimmunoprecipitation

Treated cells were lysed in lysis buffer for 40 min on ice. The lysates were incubated overnight at 4 °C on a rotator with 4 μg of polyclonal NLRP3 and mouse IgG antibodies (Abcam, USA). Fifty microlitres of protein A/G beads (Biolink, Shanghai, China) were transferred to the protein–antibody complexes, and the immunoprecipitates were collected after 2 h of incubation. Finally, the immunoprecipitates were resuspended in lithium dodecyl sulfate (LDS) sample buffer and heated for 10–12 min at 70 °C for analysis by LDS polyacrylamide gel electrophoresis. Equal concentrations of protein from the original lysates were loaded onto the gels and subsequent western blotting (WB) with monoclonal antibodies against LPP (CST, American), GAPDH, and NLRP3 was carried out.

Destabilization of the medial meniscus (DMM)-induced OA model

Male wild-type (WT) C57BL/6J and NLRP3-/- mice were housed under specific pathogen-free conditions and used in experiments at 12 weeks of age. The mice were provided a normal diet and given ad libitum access to water. The mice were anaesthetised via isoflurane inhalation before the operation. Anaesthesia was induced with 2–3% isoflurane, and 1.5–2% isoflurane was then used for anaesthesia maintenance. Experimental knee OA (KOA) was induced in the mice via transection of the medial anterior meniscotibial ligament in the left knee as previously described, and sham surgery was used as a control. To exclude the osteoprotective effect of oestrogen in female mice, male mice were selected for all experiments. In brief, C57BL/6J and NLRP3-/- mice were randomly divided into four groups ($n = 5$/group): the sham operation group, DMM group, oeNC + DMM group and oeCAV1 + DMM group. After 8 weeks (weight of 17 ± 0.3 g), the mice were euthanised, and the knee joints were harvested from the mice and further analysed by HE, Safranin-fixed green dyeing and immunohistochemical analysis. We equated synovial thickening with synovitis, The degree of synovitis was scored semiquantitatively (0–3) [30].

Histological IF staining

To stain cryosections of the mouse knee joints, the samples were blocked with rat serum or 0.2% BSA and permeabilised with 0.1% saponin in PBS for 1 h at room temperature. For the IF staining, the antibodies listed in Supplementary Table 3 were used. Staining was performed for 4 h at room temperature or overnight at 4 °C using the indicated antibodies diluted in blocking solution. Unbound primary antibodies were washed off with DPBS, and unlabelled primary antibodies were counterstained with goat anti-rabbit IgG or goat anti-mouse IgG antibody in blocking solution for 4 h at room temperature and washed with DPBS. Joint sections were stained with DAPI or SYTOX Blue by incubating the samples for 10 min (DAPI) or 1 h (SYTOX Blue) at room temperature. The samples were washed three times with DPBS and once with water for injection and embedded onto a coverslip with Dako Fluorescence Mounting Medium.

Analysis of electrophoretic bands via LC–MS/MS

LC–MS/MS was performed by BGI-Tech (Shenzhen, China). Proteins were digested via trypsin (Pierce, US) at a ratio of 1:50 (w/w, trypsin: protein) for 20 h at 37 °C. The nano-LC–MS/MS experiments were performed on an HPLC system composed of 2 LC–20AD nanoflow LC

pumps, an aSIL−20 AC autosampler, and an LC−20AB microflow LC pump (all Shimadzu, Tokyo, Japan) connected to a Q-Exactive HF X mass spectrometer (Thermo Fisher, San Jose, CA). The mass spectrometry data were matched with data simulated by the Swiss-Prot/UniProt database with Mascot 2.3.02 to obtain the protein results. The Gene Ontology (GO), Clusters of Orthologous Groups of proteins (COGs), and Kyoto Encyclopedia of Genes and Genomes (KEGG) databases were used for the analysis.

Scanning electron microscopy

For high-magnification imaging of the histological joint sections, a Leica TCS SP 5 II confocal microscope with an acousto-optic tunable filter, an acousto-optic beam splitter and a hybrid detector (HyD) on a DMI6000 CS frame was used. Imaging of coverslip-embedded samples was performed using an HCX PL APO 100× oil objective with an NA of 1.44. Fluorescence signals were generated via sequential scans, with tdTomato excitation using a diode-pumped solid-state laser at 561 nm and detection with a HyD at 600–650 nm. A second imaging sequence for visualizing Alexa Fluor 488- or FITC-labelled staining included the use of an argon laser at 488 nm for excitation and a HyD detector at 500–550 nm. The third imaging sequence involved simultaneous excitation of SYTOX Blue with a 458-nm argon laser and Alexa Fluor 647 staining with a 633-nm helium-neon laser. SYTOX Blue was detected with a HyD detector at 470–520 nm, and the Alexa Fluor signals were detected with a HyD detector at 650–700 nm. The generated images were deconvoluted with Huygens Professional and 3D-reconstructed with Imaris software.

Statistical analysis

All the experiments were performed with three or more biological replicates. All experiments were subjected to a normal distribution test. For those that followed a normal distribution, we used a t-test. For those that did not follow a normal distribution, we performed the Mann Whitney U test. The data are expressed as the mean ± standard deviation (SD). One-way analysis of variance (ANOVA) and the Kruskal–Wallis test were carried out for comparisons among multiple groups. Data analysis was performed via SPSS version 20 (IBM Corporation, Armonk, NY, United States). Differences for which $p < 0.05$ were considered significant.

Results

NLRP3 inflammasome-mediated pyroptosis in OA-FLSs is triggered by the endocytosis of chondrocyte lysates

To explore the role of NLRP3 inflammasome-induced pyroptosis in synovitis and OA, we first examined the expression level of NLRP3 in FLSs and the synovium. The mRNA and protein levels of NLRP3 were significantly increased in synovial tissues collected from OA patients (Figs. 1A, B; Figures S1A-C). NLRP3 expression was also increased in FLSs from OA synovial tissues in vivo, as verified by double immunostaining for NLRP3 and vimentin (a specific marker of fibroblasts) (Fig. 1C). The immunohistochemical staining of NLRP3 in the synovium of patients with and without OA was also consistent with previous results (Figure S2A). Moreover, we isolated FLSs from normal articular (NA) and OA synovial tissue and discovered that the NLRP3 levels were also elevated in OA-FLSs in vitro (Fig. 1D). These findings suggest dramatically elevated NLRP3 levels and enhanced subsequent pyroptosis in OA-FLSs compared with those in normal FLSs.

Next, we sought to determine the effect of cartilage CLs on FLS pyroptosis. We isolated primary chondrocytes, lysed them to form CLs and cocultured the CLs with FLSs. Surprisingly, in addition to the NLRP3 level, the mRNA levels of IL-1β, IL-18 and TNF-α, proinflammatory cytokines that are specifically secreted during pyroptosis [31], were also elevated in FLSs upon CL pretreatment (Fig. 1E). Additionally, the protein levels of IL-1β, IL-18, and NLRP3 and the pyroptosis-related proteins caspase-1 and GSDMD were significantly increased (Fig. 1F). More importantly, to determine whether CLs are internalised by FLSs, we coimmunostained CLs and NLRP3 in FLSs. Confocal imaging of CLs labelled with Cy5 revealed that CLs were phagocytised by FLSs and that NLRP3 expression was upregulated in FLSs (Fig. 1G). Moreover, we examined its effect on FLS homeostasis via flow cytometry and TUNEL. IL-1β secreted by FLSs was elevated after CL coculture (Fig. 2A). TUNEL staining and flow cytometry revealed that the pyroptosis rate of FLSs was significantly increased (Figs. 2B, C). Similarly, the results of the CCK-8 assay revealed that CL coculture impaired FLS viability (Fig. 2D). The results from the cell cycle analysis revealed that the proportion of FLSs in the G2-M phase was prolonged, suggesting that the FLSs pretreated with CLs experienced cell cycle arrest (Fig. 2E). Moreover, we observed an extreme increase in the level of perforation of the cellular membrane, a classic marker used to identify pyroptosis, compared with that in FLSs without CL pretreatment by scanning electron microscopy (SEM) (Fig. 2F). Similar effects were also observed in the Raw264.7 cell line, which is a classic cell line that resembles macrophages, treated with CLs (Figure S2C). In addition, transmission electron microscopy (TEM) revealed aberrant mitochondrial swelling in FLSs (Figure S2B). Taken together, these results suggest that CL engulfment by FLSs is closely related to NLRP3 inflammasome-induced pyroptosis and synovitis.

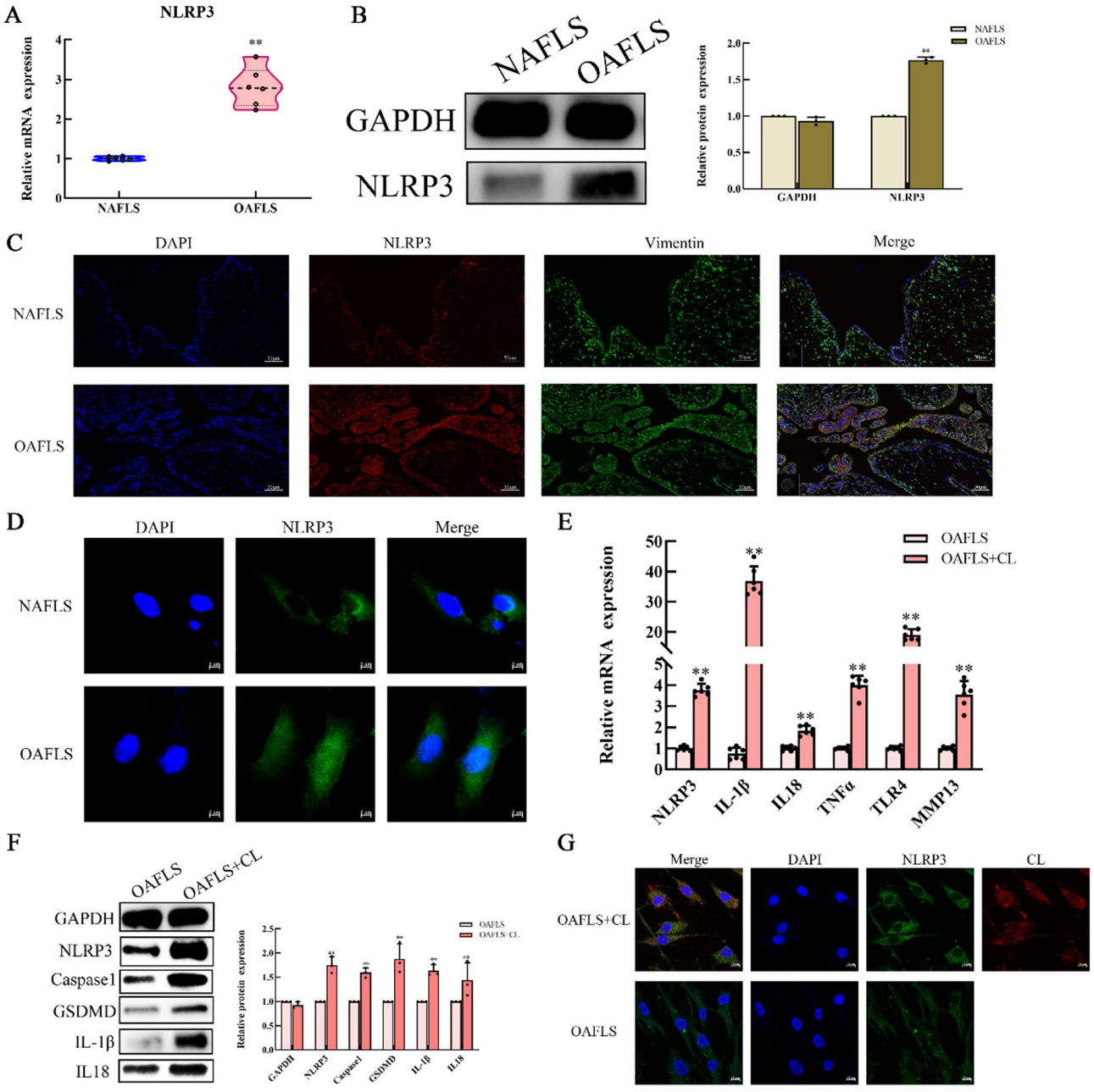

Fig. 1 Chondrocyte lysates upregulate the expression of NLRP3 via endocytosis by FLSs. (**A**). Quantitative PCR analysis of NLRP3 in primary FLSs from normal articular (NA) tissue and OA tissue ($n=6$). (**B**) WB analysis of NLRP3 in synovium obtained from individuals with NA and from patients with OA ($n=3$). (**C**) Representative coimmunofluorescence images of NLRP3 (red fluorescence) and vimentin (green fluorescence), a marker of FLSs, in synovial tissues harvested from NA and OA patients. A scale bar is presented in each image for precision. (**D**) Immunostaining of NLRP3 (green light) in primary FLSs isolated from NA and OA patients. (**E**) qRT–PCR for NLRP3, IL-1β, IL-18, TNF-α, TLR4 and MMP13 in FLSs with or without CL pretreatment. (**F**) WB analysis of NLRP3, caspase-1, GSDMD, IL-1β, and IL-18 in FLSs with and without CL stimulation. (**G**) Representative images of coimmunostaining for NLRP3 (green fluorescence) and CLs (red fluorescence) in FLSs with and without CL pretreatment. All the data are presented as the means ± SEMs. Paired t tests and one-way analysis of variance (ANOVA) were used for statistical analysis. * $p<0.05$, ** $p<0.01$, ***$p<0.001$. FLSs, fibroblast-like synoviocytes; NA, normal articular; OA, osteoarthritis

Chondrocyte lysate-stimulated FLSs regulate the anabolism and catabolism of chondrocytes

We next sought to investigate whether chondrocytes were affected by FLSs after CL coculture. We isolated primary chondrocytes from patients with OA. Then, FLSs with or without CL treatment were cocultured with primary human chondrocytes for 24 h. qRT–PCR and WB analysis confirmed that the expression of type II collagen (COL2A1) was lower and that of MMP13 was greater in chondrocytes cocultured with FLSs subjected to CL

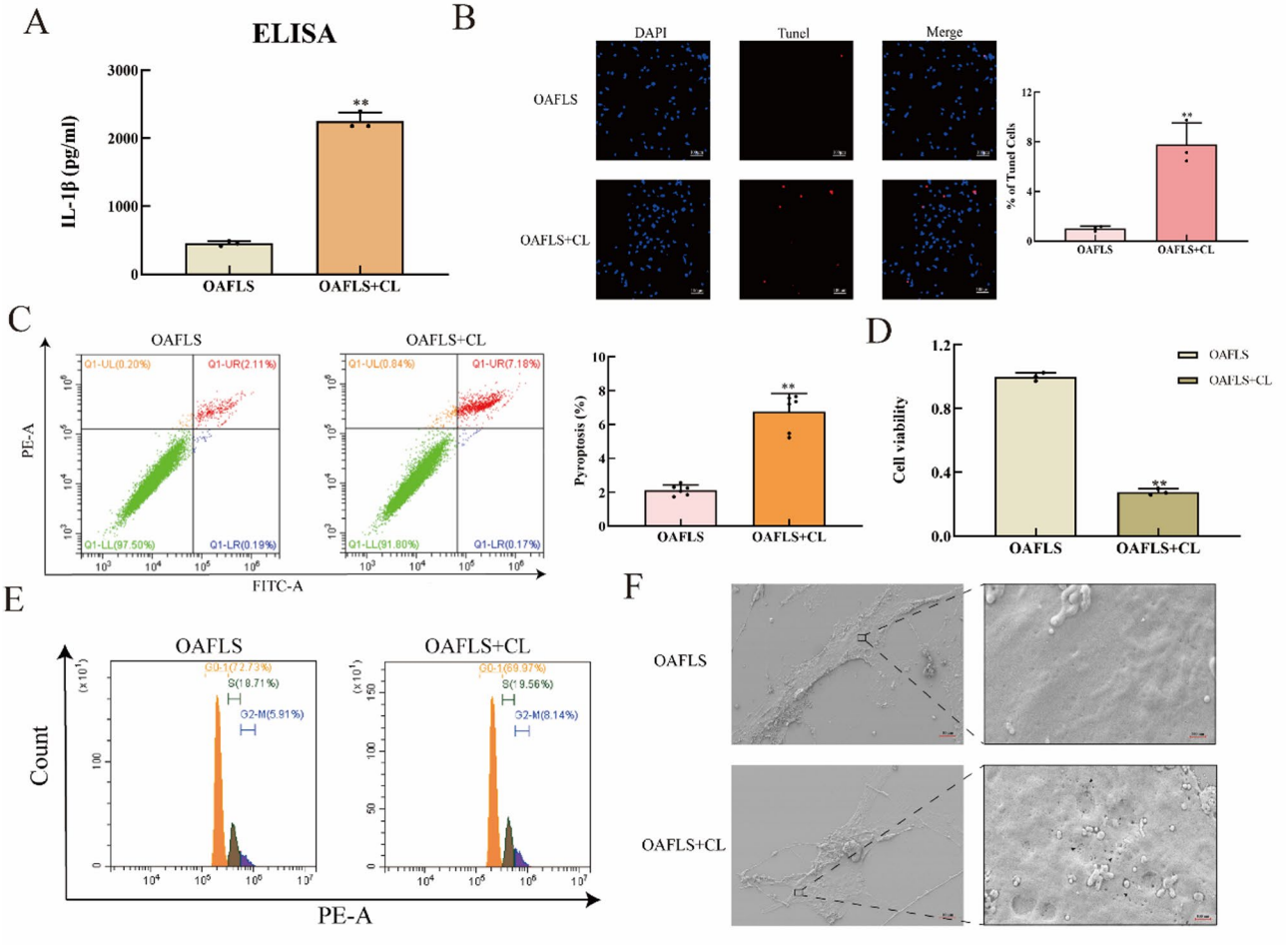

Fig. 2 Chondrocyte lysates promote the secretion of inflammatory cytokines by enhancing pyroptosis in FLSs. (**A**) ELISA of the protein levels of IL-1β in the cell supernatants of primary FLSs with or without CL treatment. (**B**). Representative images of TUNEL-stained primary FLSs with or without CL treatment and quantification of the percentage of TdT-positive cells ($n = 3$). A scale bar is presented in each image for precision. (**C**). The pyroptotic rates of FLSs with or without CL pretreatment were detected via flow cytometry via Annexin V-FITC/PI double staining and quantified via FACS analysis. (**D**). The viability of FLSs with and without CL pretreatment was quantified via the CCK-8 assay. (**E**). The effect of CLs on the cell cycle of FLSs was detected by flow cytometry and PI staining. (**F**). Representative SEM images focused on the perforation of the cellular membrane on FLSs with and without CL pretreatment. All the data are presented as the means ± SEMs. Paired t tests and one-way analysis of variance (ANOVA) were used for statistical analysis. * $p < 0.05$, ** $p < 0.01$, ***$p < 0.001$. A scale bar is presented in each image for precision. FLSs, fibroblast-like synoviocytes;

treatment (Figures S3A, B). Hence, in turn, FLSs engulfed CLs, which also promoted chondrocyte catabolism and contributed to cartilage degeneration, indicating the crucial roles of CLs and FLSs in OA.

Chondrocyte lysates downregulate the expression of CAV1 in FLSs via CAV1-dependent endocytosis during synovitis

After confirming that CLs are engulfed by FLSs via endocytosis, thereby activating NLRP3 inflammasome-mediated pyroptosis and aggravating cartilage degeneration, we sought to explore how CLs are engulfed by FLSs. Previous studies have suggested that CAV1, a major component of caveolae membranes, can regulate endocytosis in multiple cell types. Hence, we hypothesised that CAV1 acts as an important mediator of FLS-mediated endocytosis of CLs. First, qRT–PCR and WB analyses confirmed that the expression of CAV1 was significantly downregulated in FLSs treated with CLs (Figs. 3A, B). In addition, the expression of CAV1 in patients with and without OA was confirmed via qRT–PCR, WB and IF staining in vitro and in vivo, and the results suggested that the expression of CAV1 was also suppressed in the synovium and FLSs of patients with OA (Figures S4A-D). IF staining further revealed that CLs were internalised by FLSs and suppressed the expression of CAV1, suggesting that CLs regulated the expression of CAV1 after being consumed by FLSs (Fig. 3C). To prove that CLs were consumed by FLSs via CAV1-regulated endocytosis, we constructed a small-interfering RNA specific for CAV1 and transfected it into FLSs. The effect of CAV1 knockdown by siRNA was demonstrated via qRT–PCR (Figure S5). Confocal SEM revealed increased enrichment of CLs in

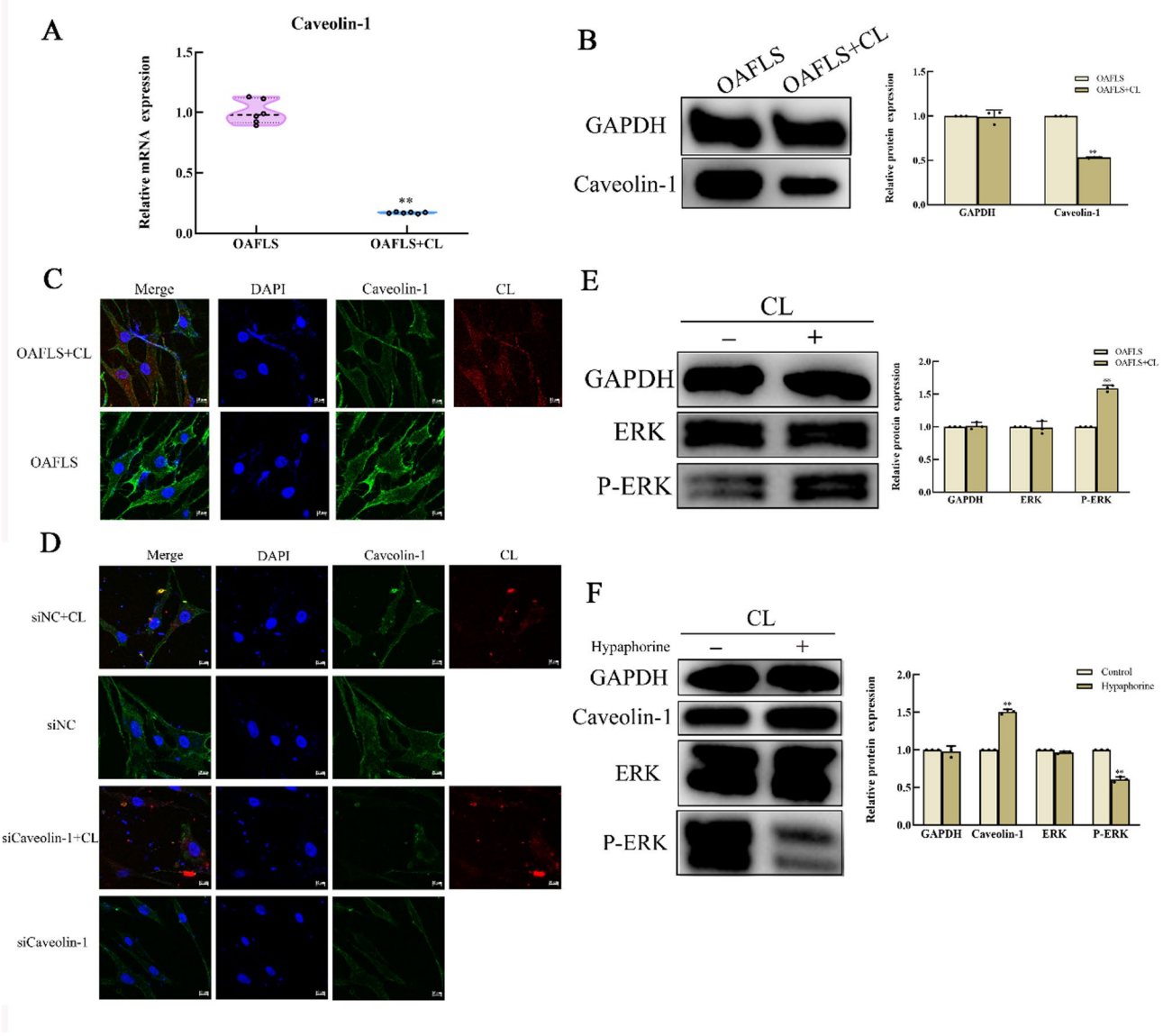

Fig. 3 The endocytosis of chondrocyte lysates by FLSs is regulated through CAV1, and CLs downregulate the expression of CAV1 in FLSs. (**A**). qRT–PCR analysis of CAV1 in FLSs with and without CL pretreatment ($n=6$). (**B**). WB and quantification of CAV1 levels in FLSs with or without CL pretreatment ($n=3$). (**C**). Representative coimmunofluorescence images of CAV1 (green fluorescence) and CLs (red fluorescence). (**D**). Representative coimmunostaining images for CAV1 and NLRP3 in FLSs with or without CL pretreatment after transfection with si-CAV1 or a control. (**E**). WB and quantitative analysis of ERK and p-ERK levels in FLSs with or without CL pretreatment. (**F**). WB and quantitative analysis of CAV1, ERK and p-ERK levels in CL-stimulated FLSs with or without hypaphorine treatment ($n=3$). All the data are presented as the means ± SEMs. Paired t tests and one-way analysis of variance (ANOVA) were used for statistical analysis. * $p<0.05$, ** $p<0.01$, *** $p<0.001$. FLSs, fibroblast-like synoviocytes; NA, normal articular; OA, osteoarthritis

the cytoplasm of FLSs after CAV1 knockdown following CL treatment (Fig. 3D). These results suggested that the endocytosis of CLs by FLSs was regulated by CAV1 and that the expression of CAV1 was further suppressed by CL treatment. Afterwards, we explored the potential mechanism underlying this process. The suppression of CAV1 was reported to be activated by ERK phosphorylation, and the TLR4 pathway might also regulate the level of CAV1 [32, 33]. Hence, we aimed to determine whether the ERK1/2 or TLR4 pathway regulates the expression of CAV1 in FLSs treated with CLs. WB analysis indicated that CL administration increased ERK1/2 phosphorylation (Fig. 3E). The protein level of Toll-like receptor 4 (TLR4) was also significantly increased in CL-stimulated FLSs (Figure S6A). Moreover, hypaphorine, an established inhibitor of ERK1/2 phosphorylation, rescued the protein level of CAV1 under CL stimulation (Fig. 3F). We also constructed siRNAs to knock down TLR4 and analysed the effects of siTLR4#002 on the expression of TLR4 and several pyroptotic markers (Figures S6 B, C). TLR4 knockdown in vitro after CL administration also upregulated the expression of CAV1, which was accompanied by

the elevated expression of several pyroptotic markers (IL-1β, IL-18, NLRP3, and TNF-α) and the downregulation of MMP13. These results suggest that CL endocytosis by FLSs is regulated by CAV1, while CLs inhibit the expression of CAV1 in FLSs via ERK phosphorylation and the TLR4 pathway.

CAV1 regulates NLRP3 inflammasome-mediated pyroptosis in FLSs

In addition to regulating CL endocytosis, we evaluated the effect of CAV1 on NLRP3 inflammasome-mediated pyroptosis in FLSs. We constructed a siRNA against CAV1 and transfected it into FLSs. qRT−PCR revealed that CAV1 knockdown significantly increased the expression levels of several inflammatory factors, such as IL-1β, IL-18, TNF-α, NLRP3 and MMP13, in FLSs (Fig. 4A). The protein levels of caspase-1 and NLRP3 were greater after CAV1 knockdown (Fig. 4B). Under CL stimulation, CAV1 inhibition contributed to increased levels of pyroptosis (Fig. 4C). In vitro double immunostaining for CAV1 and NLRP3 revealed that CAV1 inhibition profoundly promoted NLRP3 expression with or without CL administration (Fig. 4D). Flow cytometry further confirmed that CAV1 silencing promoted pyroptosis in FLSs (Fig. 4E). Moreover, CAV1 silencing enhanced the inflammatory phenotype of FLSs, as confirmed by the level of IL-1β secreted by FLSs as detected by ELISA (Fig. 4F).

Furthermore, we constructed a plasmid encoding CAV1 and transfected it into FLSs to evaluate the effect of CAV1 on NLRP3 inflammasome-mediated pyroptosis. qRT−PCR indicated that CAV1 overexpression suppressed the expression of IL-18, NLRP3 and MMP13 (Figure S7A). On the other hand, the expression levels of IL-1β and TNF-α were elevated after CAV1 overexpression, but the extent of this upregulation was lower than that in FLSs treated with CLs (Figure S7C). WB revealed that CAV1 overexpression decreased the protein levels of caspase-1 and NLRP3 (Figure S7B). IF staining of NLRP3 and CAV1 in vitro revealed that CLs promoted pyroptosis in FLSs and that CAV1 rescued pyroptosis (Figure S7D). Moreover, in contrast with CAV1 silencing, CAV1 overexpression alleviated pyroptosis and suppressed IL-1β secretion in FLSs (Figures S7E, F). Taken together, these results suggest that under CL treatment, CAV1 modulates NLRP3 inflammasome-mediated pyroptosis and the inflammatory phenotype in FLSs.

CAV1 overexpression alleviates synovitis through NLRP3 in mice with DMM-induced OA

To prove that CAV1 plays an important role in regulating NLRP3 inflammasome-mediated pyroptosis in FLSs and synovitis in vivo, we performed DMM surgery to establish OA models in WT and NLRP3 knockout (NLRP3-/-) mice. Moreover, intra-articular injection of AAV expressing CAV1 was performed once a week. Agarose gel electrophoresis confirmed that NLRP3 in NLRP3-/- mice marked 1,2,3,5,6,7,8,9,11, 12,13,15,17,18 and 19 had been successfully deleted (Figure S8A), and IF staining again confirmed that NLRP3 in NLRP3-/- mice had been successfully deleted (Figure S8B). HE staining revealed that AAV-CAV1 alleviated the synovial hyperplasia in the DMM mice, and similarly, the NLRP3-/- mice also presented a lower extent of synovial hyperplasia and inflammation after DMM surgery than did the WT mice (Fig. 5A). However, no significant change in the synovium was observed between the NLRP3-/- DMM + oeCAV1 group and the NLRP3-/- DMM + oeNC group, indicating that CAV1 alleviates synovitis via NLRP3 inflammasome-mediated pyroptosis (Fig. 5A). The synovitis scores of all the samples were quantified. Coimmunofluorescence analysis of vimentin and CAV1 confirmed that the AAV was successfully injected into the knee joint and that CAV1 was overexpressed in FLSs residing in the synovium (Figs. 5B, C). Consistently, the expression level of NLRP3 was significantly lower in the DMM model mice treated with AAV-CAV1 than in the control mice (Fig. 5D). Previous studies have reported that CAV1 promotes cartilage destruction by activating the MAPK pathway, and our results suggest that CAV1 may play different roles in cartilage and the synovium. Hence, CAV1 rescued synovitis by modulating NLRP3 inflammasome-mediated pyroptosis in mice.

LPP in CLs induces pyroptosis in FLSs by inhibiting CAV1 expression

CLs contain various proteins that might act as regulators of homeostasis in the knee. However, the specific proteins that connect CLs and pyroptosis in FLSs remain uncertain. To identify the specific proteins that activate NLRP3 inflammasome-mediated pyroptosis in FLSs, mass spectrometry was performed to screen potential proteins in CLs harvested from three patients with OA. Coimmunoprecipitation (co-IP) was also carried out to identify NLRP3-binding proteins after FLSs were stimulated with CLs. The proteins pulled down from NLRP3 were also subjected to mass spectrometry. Afterwards, we compared the results to determine the specific proteins that were not only present in the CLs but also bound to NLRP3 in the FLSs. Only LPP was identified as a potential regulator in CLs that might be transferred to FLSs to activate NLRP3 inflammasome pyroptosis (Fig. 6A). Co-IP confirmed that the level of LPP pulled from NLRP3 was significantly greater after CL stimulation (Fig. 6B). On the basis of these results, we further evaluated whether LPP regulated pyroptosis in FLSs. As expected, the recombinant LPP protein markedly elevated the expression levels of several inflammatory cytokines, such

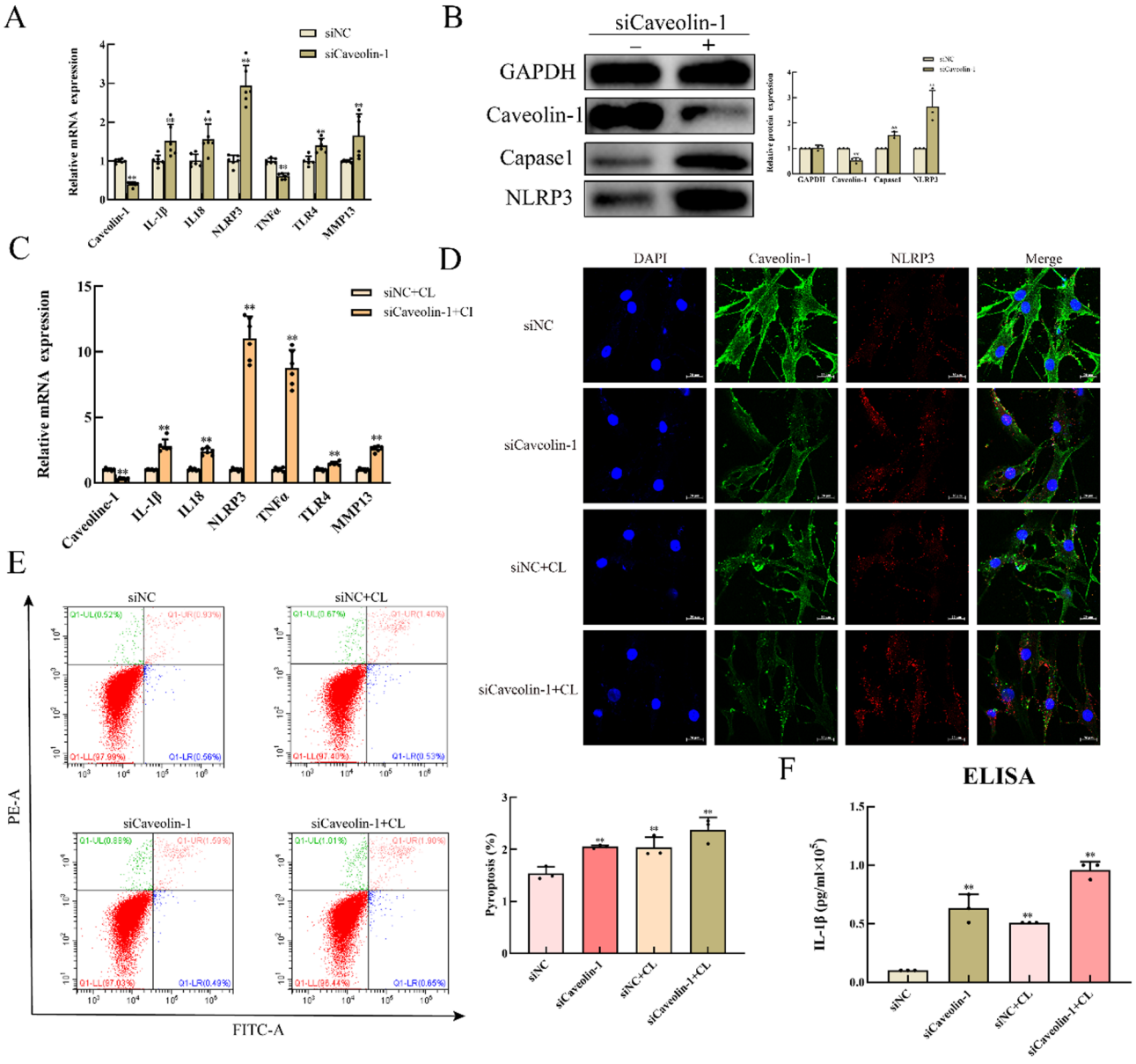

Fig. 4 Silencing CAV1 in FLSs in vitro promotes NLRP3 inflammasome-mediated pyroptosis and is associated with synovitis. (**A**). qRT–PCR of CAV1, IL-1β, IL-18, NLRP3, TNF-α, TLR4, and MMP13 in FLSs transfected with si-CAV1 for 2 days or transfected with the control ($n=6$). (**B**). WB and quantification of CAV1, caspase-1 and NLRP3 levels after transfection with si-CAV1 for 3 days or after transfection with the control ($n=3$). (**C**). qRT–PCR analysis of CAV1, IL-1β, IL-18, NLRP3, TNF-α, TLR4, and MMP13 in CL-stimulated FLSs after transfection with si-CAV1 for 2 days or the control ($n=3$). (**D**). Representative images of coimmunostaining for CAV1 and NLRP3 in FLSs with or without CL pretreatment after transfection with si-CAV1 or the control. (**E**). The rates of pyroptosis were analysed via flow cytometry via Annexin V-FITC/PI double staining, and the number of pyroptotic cells was determined via FACS. (**F**). ELISA was used to detect the concentration of IL-1β in the cell supernatants of FLSs treated with CLs and si-CAV1 or the control ($n=3$). All the data are presented as the means ± SEMs. Paired t tests and one-way analysis of variance (ANOVA) were used for statistical analysis. * $p<0.05$, ** $p<0.01$, ***$p<0.001$

as IL-1β, IL-18, TNF-α, MMP13 and NLRP3, but downregulated CAV1 expression (Fig. 6C). The WB results were consistent with the qRT–PCR results in terms of the levels of CAV1 and NLRP3 after incubation with LPP (Fig. 6D). Flow cytometry also revealed a greater pyroptotic rate in FLSs treated with LPP than in the control groups (Fig. 6E). Similarly, IF staining confirmed that the recombinant LPP protein suppressed CAV1 expression and upregulated NLRP3 expression in FLSs (Fig. 6F). In conclusion, the CL-specific protein LPP promotes NLRP3 inflammasome-mediated pyroptosis and synovitis by inhibiting CAV1 expression in FLSs.

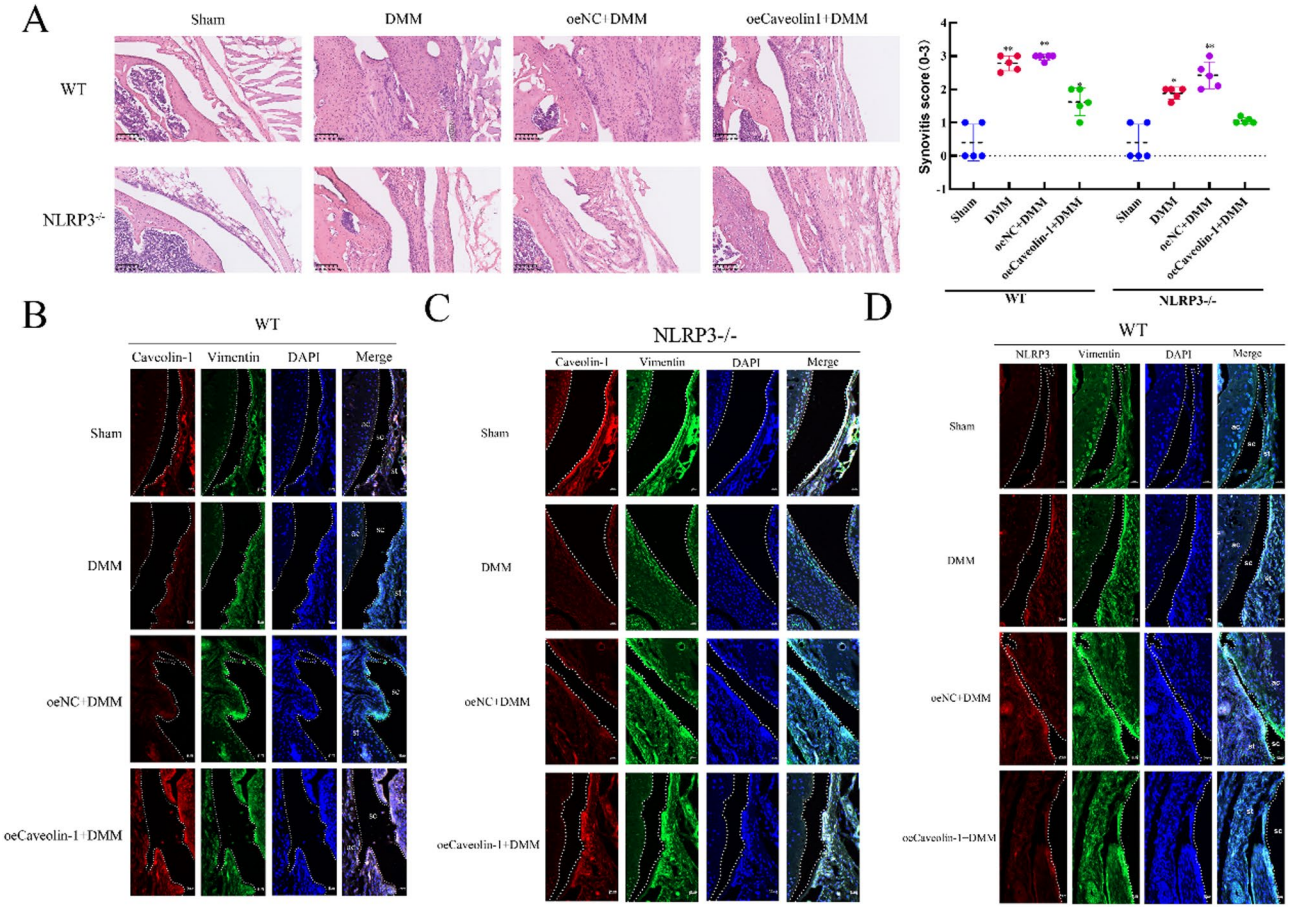

Fig. 5 CAV1 overexpression in FLSs alleviates synovitis in a DMM-induced OA model through the regulation of NLRP3 inflammasome-mediated pyroptosis. (**A**). Representative images of HE-stained knee joints from C57BL/6J (wild-type) DMM mice and NLRP3 knockout DMM mice with or without intra-articular injection of AAV-CAV1 (oeCAV1) and quantification of the synovitis score ($n = 5$). (**B**). Representative images of coimmunofluorescence of CAV1 (red fluorescence) and vimentin (green fluorescence) in knee joints from C57BL/6J (wild-type) DMM mice with or without intra-articular injection of AAV-CAV1 ($n = 5$). (**C**). Representative images of NLRP3 (red fluorescence) and vimentin (green fluorescence) in knee joints from C57BL/6J (wild-type) DMM mice with or without intra-articular injection of AAV-CAV1 ($n = 5$). (**D**). Representative images of coimmunofluorescence of CAV1 (red fluorescence) and vimentin (green fluorescence) in the knee joints of NLRP3 knockout mice with or without intra-articular injection of AAV-CAV1 ($n = 5$). All the data are presented as the means ± SEMs. Paired t tests and one-way analysis of variance (ANOVA) were used for statistical analysis. * $p < 0.05$, ** $p < 0.01$, *** $p < 0.001$. HE, haematoxylin–eosin; DMM, destabilization of the medial meniscus; AAV, adeno-associated virus. KO, knockout

Discussion

OA, which is characterised by cartilage destruction, osteophyte formation, and synovial hyperplasia, is an age-related or posttraumatic disease with very high morbidity in the elderly population [34]. The synovium plays an important role in maintaining joint homeostasis. Furthermore, it contributes to degeneration of the joint in OA by releasing inflammatory molecules [35, 36]. Our research revealed that CLs can aggravate synovial inflammation, indicating that they play an important role in the pathogenesis of OA, which is consistent with previous research [37]. The NLRP3 inflammasome is involved in the development of OA, leading to the degradation of cartilage and synovial inflammation [38]. In this study, we found that the expression of NLRP3 was significantly lower in the synovium of normal controls than in that of OA patients and that the expression of NLRP3 increased after OA-FLSs were stimulated with CLs, which is consistent with the findings of a previous study [39]. Some studies have reported that CAV1 is highly expressed in cartilage [28, 40], but there are few reports on CAV1 in synovial cells. Our experiments revealed that, in contrast to that in cartilage, the expression of CAV1 in the synovium of normal individuals was significantly higher than that in OA patients, and the expression of CAV1 was significantly lower after stimulation with CLs. CAV1 may interact with the NLRP3 inflammasome to affect synovial inflammation caused by CLs, according to our findings. Therefore, clarifying the relevant mechanisms may provide potential targets for the treatment of early OA.

Recently, pyroptosis, a method of programmed cell death, has been reported in multiple diseases. Pyroptosis

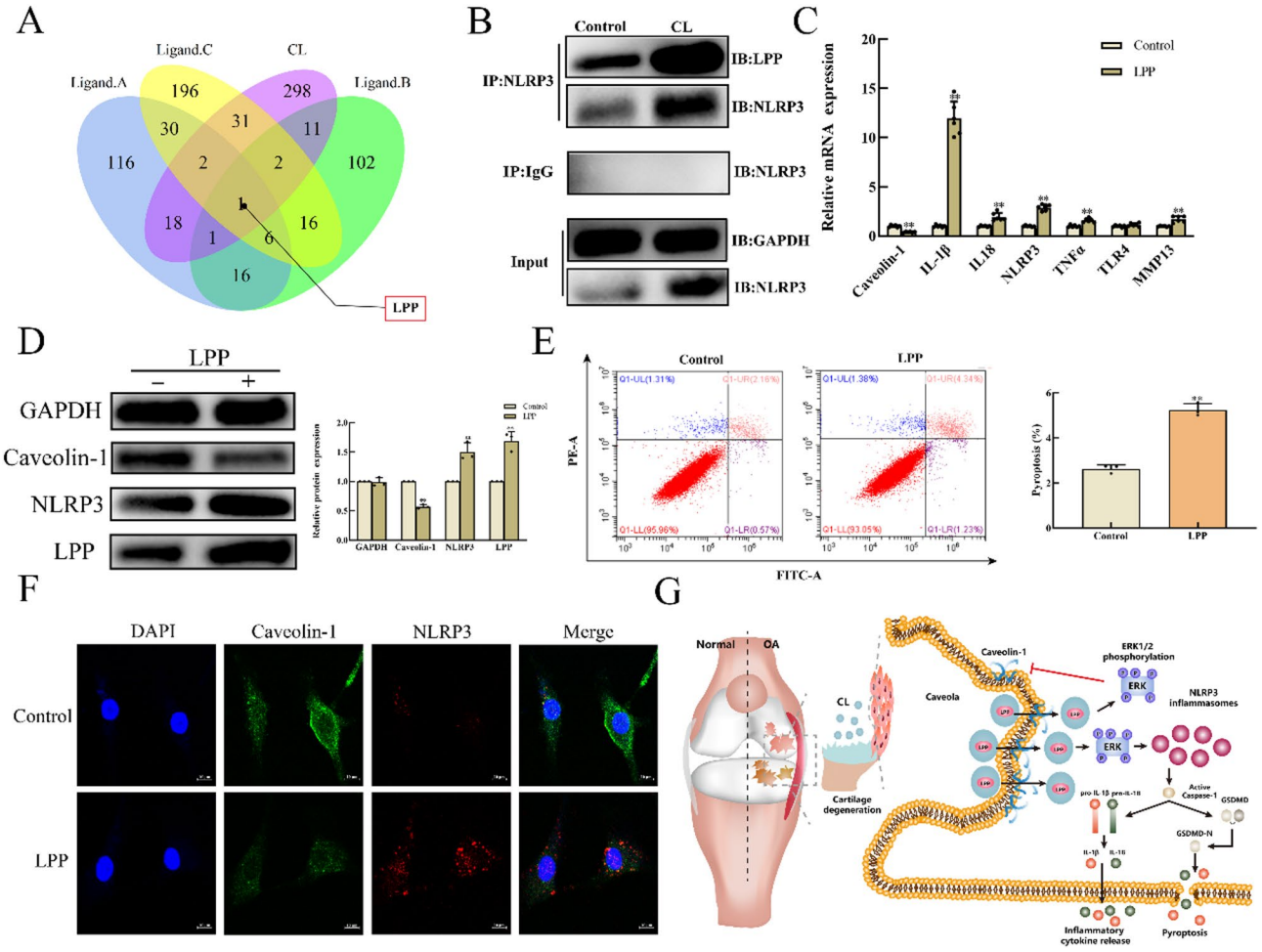

Fig. 6 LPP in chondrocyte lysates promotes NLRP3 inflammasome-mediated pyroptosis in FLSs. (**A**). Venn diagram of screened proteins detected by LC–MS from CLs and FLSs isolated from 3 different groups (Ligand A/B/C) of OA patients with CL stimulation. (**B**). Co-IP analysis of LPP pulled down from NLRP3 in FLSs with or without CL pretreatment. (**C**). qRT–PCR analysis of CAV1, IL-1β, IL-18, NLRP3, TNF-α, TLR4, and MMP13 levels in cells with or without recombinant LPP protein treatment ($n=6$). (**D**). WB and quantification of CAV1, NLRP3, and LPP levels in FLSs with and without LPP treatment. (**E**). The pyroptotic rates of FLSs with and without recombinant LPP protein treatment were quantified via flow cytometry with double Annexin V-FITC/PI staining ($n=3$). (**F**). Representative images of the coimmunofluorescence of CAV1 (green fluorescence) and NLRP3 (red fluorescence) with and without LPP treatment are shown. (**G**). Schematic representation of the mechanisms by which CLs regulate synovitis. All the data are presented as the means ± SEMs. Paired t tests and one-way analysis of variance (ANOVA) were used for statistical analysis. * $p<0.05$, ** $p<0.01$, ***$p<0.001$. LC–MS

is caused mainly by the activation of caspases, which cut the junction between the N-terminal and C-terminal domains of the GSDMD protein and release the N-terminal domain, which has membrane-perforating activity at the membrane phospholipid and destroys the cell membrane to cause pyrosis, cell lysis and IL-1β release [41, 42]. In inflammatory diseases, this process can cause an inflammatory cascade via further activation of resident cells and recruitment of more inflammatory cells [43]. NLRP3 inflammasome-mediated synoviocyte pyroptosis has been reported to be involved in the progression of KOA [8, 44–46]. In this study, we found that NLRP3 was highly expressed in human OA synovial tissue, where it acts as a proinflammatory medium, and that when caspase-1 and IL-1β were added after CLs, the IL-18 and GSDMD levels were significantly increased, cell apoptosis was increased, and cell membrane perforation was observed via SEM. Therefore, we showed that the NLRP3 inflammatory corpuscle is involved in the pathogenesis of synovitis in OA patients.

In addition to its participation in the formation of caveolae, CAV1 directly interacts with multiple signalling proteins via its scaffolding domain to regulate their activity. These proteins are important regulators of cell transformation and growth [47]. Previous reports have demonstrated that CAV1 overexpression results in cellular senescence in chondrocytes, whereas a reduction in CAV1 levels in senescent chondrocytes can modify the ageing phenotype [48]. Our data revealed that the expression of CAV1 in OA patient synovium was significantly

lower than that in normal control synovium and that the expression of CAV1 in the OA synovium was reduced after CL stimulation. The anti-inflammatory effects of CAV1 are mediated by its binding and inactivation of ERK1/2, PI3-K and PKA [49, 50]. This finding is in line with our observations that ERK phosphorylation was activated after the addition of CLs, and the expression of CAV1 and NLRP3 increased after the addition of an ERK inhibitor. As a result, we hypothesise that CAV1 can regulate FLS pyrosis via the ERK pathway.

We found that in vitro silencing and overexpression of CAV1 also affected NLRP3-mediated pyroptosis. A decrease in CAV1 can activate the formation of NLRP3 inflammatory bodies, and an increase in CAV1 can inhibit the death of synovial fibroblasts. CAV1 overexpression in vivo decreased the expression of NLRP3 in synovial cells and inhibited the proliferation of cells in the synovial membrane. However, after CAV1 was overexpressed in cartilage, osteophyte hyperplasia and cartilage destruction increased.

These findings suggest that CAV1 regulates the pyroptosis of CL-activated FSLs. We analysed CL-stimulated FLSs via mass spectrometry and co-IP. The results revealed that LPP was the only protein identified by both methods. The LPP protein is a member of the zyxin family of LIM domain proteins and is located at sites of cell adhesion and cell–cell contact [51, 52]. In addition, it interacts with α-actinin (ACTN1) to participate in diverse cellular processes, such as cell adhesion, spreading and migration [53]. LPP may partner with different molecules, which reflects its various functions; therefore, LPP may act as a potential oncogene or onco-suppressor gene in different cancer cell lines [54]. The role of LPP in arthritic joint tissue has rarely been reported. We used the LPP protein to stimulate OA-FLSs and verified that the effect of LPP was similar to that of CLs, as both could stimulate OA-FLSs; therefore, we hypothesise that LPP is the main substance in CLs that decreases CAV1 levels.

However, several limitations need to be addressed. First, because it is difficult to obtain normal synovial tissue from elderly individuals, we chose specimens obtained from young arthroscopic patients (mostly males and those suffering from sports-related injuries) as the control NA; thus, this study has certain limitations. Second, more in vivo studies are needed; for example, whether the construction of CAV1 knockout mice or the addition of the LPP protein to the synovium of mice inhibits the development of OA in mice should be tested. More importantly, more in-depth research is needed to determine the potential mechanism by which CLs regulate pyroptosis. Only in this way can we treat synovitis accurately and efficiently. Furthermore, more OA patients with synovitis must be registered in a database to determine the relationship between CAV1 levels in cartilage and the synovium and OA prognosis. Moreover, overexpressing CAV1 in vivo might accelerate cartilage degeneration in vivo, which is consistent with the findings of previous studies. These contradictory findings may be due to the low precision of AAV injection, since all tissues in the knee joints were transfected with AAV-CAV1. Therefore, it is necessary to understand the underlying mechanism and discover more precise targeted therapeutic strategies to address this issue; for example, CAV1 could be specifically overexpressed in FLSs. We also need to investigate whether CAV1 expression at a threshold level can affect the microenvironment of the entire joint.

Conclusion

In conclusion, our findings reveal a new mechanism by which CLs exacerbate synovitis during cartilage injury or degeneration. Specifically, CLs promote NLRP3 inflammasome-mediated pyroptosis in FLS via CAV1-regulated endocytosis, with the LPP protein in CLs acting as a key mediator. Our study highlights the importance of CLs in promoting the exacerbation of synovitis, providing new insights into the mechanisms by which cartilage injury or degeneration can regulate synovitis and identifying therapeutic targets for the treatment of synovial inflammation.

Supplementary Information

The online version contains supplementary material available at https://doi.org/10.1186/s13075-025-03573-0.

Supplementary Material 1

Supplementary Material 2

Acknowledgements

The authors thank Professor Xuerong Li (Department of the Zhongshan School of Medicine, Sun Yat-sen University) for their technical assistance and Doctor Zhiwen Li, Xiaoyi Zhao and Guiwu Huang (Department of Joint Surgery, the First Affiliated Hospital of SunYat-sen University) for providing the cases.

The animal experiments performed in the present study adhered to protocols approved by the Institutional Review Board of Sun Yat-sen University (SYSU-IACUC-2020-000504). Male wild-type (WT) C57BL/6J mice (purchased from GemPharmatech Co., Jiangsu, China) and NLRP3-/- mice were obtained from Professor Zhongdao Wu's laboratory.

Author contributions

X.D., R N L and Z.Q.Z. were involved in the conception and design of the study. X.D. and Z.R.J. performed the immunohistochemistry assays. X.D. acquired, analysed and interpreted the data. R.N.L. and C.Y.Z. performed the animal surgeries on the mouse knee joints. X.D. performed the histologic staining of the knee joints. Z.J.Y. and S.H. performed the statistical analyses. All the authors were involved in drafting, revising and approving the final version of the manuscript.

Funding

This study was funded by the National Natural Science Foundation of China (82172467, 82202735,), the Guangdong Natural Science Funds for Distinguished Young Scholars of China (2021B1515020008), the First Affiliated Hospital of Sun Yat-sen University Ke Ling Funding Program for Novel and Distinguished Talents (R07005), the Natural Science Foundation of Guangdong Province of China (2023A1515010142, 2024A1515011189), and Shandong Provincial Natural Science Foundation (ZR2024QH552).

Data availability
No datasets were generated or analysed during the current study.

Declarations

Ethics approval and consent to participate
All experiments involving animal and patient samples in this study adhered to ethical policies and procedures approved by the Ethics Committee of the First Affiliated Hospital of Sun Yat-Sen University, China. (Approval no. IRB: IIT-2021-667; SYSU-IACUC-2020-000504).

Consent for publication
Written informed consent for publication was obtained from all participants.

Competing interests
The authors declare no competing interests.

Author details
[1]Department of Joint Surgery, First Affiliated Hospital of Sun Yat-sen University, Guangzhou 510080, Guangdong, China
[2]Department of Joint Surgery, Third Affiliated Hospital of Southern Medical University, Guangzhou, China
[3]Department of Reproductive Medicine, Affiliated Hospital of Shandong Second Medical University, Shandong, China
[4]Guangdong Provincial Key Laboratory of Orthopedics and Traumatology, First Affiliated Hospital of Sun Yat-sen University, Guangzhou 510080, Guangdong, China
[5]Guangdong Provincial Key Laboratory of Bone and Joint Degeneration Diseases, Guangzhou, China
[6]The Third School of Clinical Medicine, Southern Medical University, Guangzhou, China
[7]Department of Joint Surgery and Sports Medicine, The Third Affiliated Hospital of Southern Medical University, Shandong, China

Received: 16 February 2025 / Accepted: 6 May 2025
Published online: 15 May 2025

References

1. Yao Q, Wu X, Tao C, Gong W, Chen M, Qu M, Zhong Y, He T, Chen S, Xiao G. Osteoarthritis: pathogenic signaling pathways and therapeutic targets. Signal Transduct Target Ther. 2023;8(1):56.
2. Oppenheim JJ, Yang D. Alarmins: chemotactic activators of immune responses. Curr Opin Immunol. 2005;17(4):359–65.
3. Millerand M, Berenbaum F, Jacques C. Danger signals and inflammaging in osteoarthritis. Clin Exp Rheumatol. 2019;37(Suppl 120):48–56.
4. Nefla M, Holzinger D, Berenbaum F, Jacques C. The danger from within: alarmins in arthritis. Nat Rev Rheumatol. 2016;12(11):669–83.
5. Huang J, Xie Y, Sun X, Zeh HJ 3rd, Kang R, Lotze MT, Tang D. DAMPs, ageing, and cancer: the 'DAMP hypothesis'. Ageing Res Rev. 2015;24(Pt A):3–16.
6. Rosenberg JH, Rai V, Dilisio MF, Agrawal DK. Damage-associated molecular patterns in the pathogenesis of osteoarthritis: potentially novel therapeutic targets. Mol Cell Biochem. 2017;434(1–2):171–9.
7. Chung HY, Kim DH, Lee EK, Chung KW, Chung S, Lee B, Seo AY, Chung JH, Jung YS, Im E, et al. Redefining chronic inflammation in aging and age-related diseases: proposal of the senoinflammation concept. Aging Dis. 2019;10(2):367–82.
8. An S, Hu H, Li Y, Hu Y. Pyroptosis plays a role in osteoarthritis. Aging Dis. 2020;11(5):1146–57.
9. Christgen S, Kanneganti TD. Inflammasomes and the fine line between defense and disease. Curr Opin Immunol. 2020;62:39–44.
10. Broz P, Dixit VM. Inflammasomes: mechanism of assembly, regulation and signalling. Nat Rev Immunol. 2016;16(7):407–20.
11. Rathinam VA, Fitzgerald KA. Inflammasome complexes: emerging mechanisms and effector functions. Cell. 2016;165(4):792–800.
12. Chen C, Xu P. Activation and pharmacological regulation of inflammasomes. Biomolecules. 2022;12(7).
13. Nasi S, Ea HK, So A, Busso N. Revisiting the role of interleukin-1 pathway in osteoarthritis: interleukin-1alpha and– 1beta, and NLRP3 inflammasome are not involved in the pathological features of the murine menisectomy model of osteoarthritis. Front Pharmacol. 2017;8:282.
14. Wang Q, Onuma K, Liu C, Wong H, Bloom MS, Elliott EE, Cao RR, Hu N, Lingampalli N, Sharpe O et al. Dysregulated integrin alphaVbeta3 and CD47 signaling promotes joint inflammation, cartilage breakdown, and progression of osteoarthritis. JCI Insight. 2019;4(18).
15. Estell EG, Silverstein AM, Stefani RM, Lee AJ, Murphy LA, Shah RP, Ateshian GA, Hung CT. Cartilage wear particles induce an inflammatory response similar to cytokines in human fibroblast-like synoviocytes. J Orthop Res. 2019;37(9):1979–87.
16. Mimpen JY, Baldwin MJ, Cribbs AP, Philpott M, Carr AJ, Dakin SG, Snelling SJB. Interleukin-17A causes osteoarthritis-like transcriptional changes in human osteoarthritis-derived chondrocytes and synovial fibroblasts in vitro. Front Immunol. 2021;12:676173.
17. Rashid-Doubell F, Tannetta D, Redman CW, Sargent IL, Boyd CA, Linton EA. Caveolin-1 and lipid rafts in confluent bewo trophoblasts: evidence for Rock-1 association with caveolin-1. Placenta. 2007;28(2–3):139–51.
18. Martin S, Parton RG. Caveolin, cholesterol, and lipid bodies. Semin Cell Dev Biol. 2005;16(2):163–74.
19. Boscher C, Nabi IR. Caveolin-1: role in cell signaling. Adv Exp Med Biol. 2012;729:29–50.
20. Cheng JPX, Nichols BJ. Caveolae: one function or many?? Trends Cell Biol. 2016;26(3):177–89.
21. Yang C, He B, Dai W, Zhang H, Zheng Y, Wang X, Zhang Q. The role of caveolin-1 in the biofate and efficacy of anti-tumor drugs and their nano-drug delivery systems. Acta Pharm Sin B. 2021;11(4):961–77.
22. Jiang W, Wang J, Xue W, Xin J, Shi C, Wen J, Feng X, Huang Y, Hu C. Caveolin-1 attenuates acetaminophen aggravated lipid accumulation in alcoholic fatty liver by activating mitophagy via the Pink-1/Parkin pathway. Eur J Pharmacol. 2021;908:174324.
23. Buitrago C, Boland R. Caveolae and caveolin-1 are implicated in 1alpha,25(OH)2-vitamin D3-dependent modulation of Src, MAPK cascades and VDR localization in skeletal muscle cells. J Steroid Biochem Mol Biol. 2010;121(1–2):169–75.
24. Liu W, Jiang P, Qiu L. Blocking of caveolin-1 attenuates morphine-induced inflammation, hyperalgesia, and analgesic tolerance via inhibiting NLRP3 inflammasome and ERK/c-JUN pathway. J Mol Neurosci. 2022;72(5):1047–57.
25. Li Z, Scott MJ, Fan EK, Li Y, Liu J, Xiao G, Li S, Billiar TR, Wilson MA, Jiang Y, et al. Tissue damage negatively regulates LPS-induced macrophage necroptosis. Cell Death Differ. 2016;23(9):1428–47.
26. Jiang X, Li Y, Fu D, You T, Wu S, Xin J, Wen J, Huang Y, Hu C. Caveolin-1 ameliorates acetaminophen-aggravated inflammatory damage and lipid deposition in non-alcoholic fatty liver disease via the ROS/TXNIP/NLRP3 pathway. Int Immunopharmacol. 2023;114:109558.
27. Menzel V, Ziegler M, Hante N, Sake JA, Santos-Martinez MJ, Ehrhardt C, Kasper M, Barth K. Fyn-kinase and caveolin-1 in the alveolar epithelial junctional adherence complex contribute to the early stages of pulmonary fibrosis. Eur J Pharm Sci. 2022;175:106236.
28. Dai SM, Shan ZZ, Nakamura H, Masuko-Hongo K, Kato T, Nishioka K, Yudoh K. Catabolic stress induces features of chondrocyte senescence through overexpression of caveolin 1: possible involvement of caveolin 1-induced down-regulation of articular chondrocytes in the pathogenesis of osteoarthritis. Arthritis Rheum. 2006;54(3):818–31.
29. Chen YJ, Chang WA, Wu LY, Huang CF, Chen CH, Kuo PL. Identification of novel genes in osteoarthritic fibroblast-like synoviocytes using next-generation sequencing and bioinformatics approaches. Int J Med Sci. 2019;16(8):1057–71.
30. Baker K, Grainger A, Niu J, Clancy M, Guermazi A, Crema M, Hughes L, Buckwalter J, Wooley A, Nevitt M, et al. Relation of synovitis to knee pain using contrast-enhanced MRIs. Ann Rheum Dis. 2010;69(10):1779–83.
31. Ma J, Yang P, Zhou Z, Song T, Jia L, Ye X, et al. GYY4137-induced p65 sulfhydration protects synovial macrophages against pyroptosis by improving mitochondrial function in osteoarthritis development. J Adv Res. 2025;71:173–88.
32. Hsiao SC, Liao WH, Chang HA, Lai YS, Chan TW, Chen YC, Chiu WT. Caveolin-1 differentially regulates the transforming growth factor-beta and epidermal growth factor signaling pathways in MDCK cells. Biochim Biophys Acta Gen Subj. 2024;1868(9):130660.
33. Zhang C, Wu Q, Huang H, Chen X, Huang T, Li W, Liu Y, Zhang J. Caveolin-1 promotes Rfng expression via Erk-Jnk-p38 signaling pathway in mouse hepatocarcinoma cells. J Physiol Biochem. 2019;75(4):549–59.

34. Wu Y, Hong Z, Xu W, Chen J, Wang Q, Chen J, Ni W, Mei Z, Xie Z, Ma Y, et al. Circular RNA circPDE4D protects against osteoarthritis by binding to miR-103a-3p and regulating FGF18. Mol Ther. 2021;29(1):308–23.
35. Rahmati M, Mobasheri A, Mozafari M. Inflammatory mediators in osteoarthritis: a critical review of the state-of-the-art, current prospects, and future challenges. Bone. 2016;85:81–90.
36. Scanzello CR, Goldring SR. The role of synovitis in osteoarthritis pathogenesis. Bone. 2012;51(2):249–57.
37. Silverstein AM, Stefani RM, Sobczak E, Tong EL, Attur MG, Shah RP, Bulinski JC, Ateshian GA, Hung CT. Toward understanding the role of cartilage particulates in synovial inflammation. Osteoarthritis Cartilage. 2017;25(8):1353–61.
38. McAllister MJ, Chemaly M, Eakin AJ, Gibson DS, McGilligan VE. NLRP3 as a potentially novel biomarker for the management of osteoarthritis. Osteoarthritis Cartilage. 2018;26(5):612–9.
39. Chen Z, Zhong H, Wei J, Lin S, Zong Z, Gong F, Huang X, Sun J, Li P, Lin H, et al. Inhibition of Nrf2/HO-1 signaling leads to increased activation of the NLRP3 inflammasome in osteoarthritis. Arthritis Res Ther. 2019;21(1):300.
40. Goutas A, Papathanasiou I, Mourmoura E, Tsesmelis K, Tsezou A, Trachana V. Oxidative stress response is mediated by overexpression and spatiotemporal regulation of caveolin-1. Antioxid (Basel). 2020;9(8).
41. Ding J, Wang K, Liu W, She Y, Sun Q, Shi J, Sun H, Wang DC, Shao F. Pore-forming activity and structural autoinhibition of the gasdermin family. Nature. 2016;535(7610):111–6.
42. Van Opdenbosch N, Lamkanfi M. Caspases in cell death, inflammation, and disease. Immunity. 2019;50(6):1352–64.
43. Chan AH, Schroder K. Inflammasome signaling and regulation of interleukin-1 family cytokines. J Exp Med. 2020;217(1).
44. Zhang L, Xing R, Huang Z, Zhang N, Zhang L, Li X, Wang P. Inhibition of synovial macrophage pyroptosis alleviates synovitis and fibrosis in knee osteoarthritis. Mediators Inflamm. 2019;2019:2165918.
45. Liu X, Zhao J, Jiang H, Guo H, Li Y, Li H, Feng Y, Ke J, Long X. ALPK1 accelerates the pathogenesis of osteoarthritis by activating NLRP3 signaling. J Bone Min Res. 2022;37(10):1973–85.
46. Xin Y, Wang W, Mao E, Yang H, Li S. Targeting NLRP3 Inflammasome alleviates synovitis by reducing pyroptosis in rats with experimental temporomandibular joint osteoarthritis. Mediators Inflamm. 2022;2022:2581151.
47. van Golen KL. Is caveolin-1 a viable therapeutic target to reduce cancer metastasis? Expert Opin Ther Targets. 2006;10(5):709–21.
48. Platas J, Guillen MI, Del Perez MD, Gomar F, Castejon MA, Mirabet V, Alcaraz MJ. Paracrine effects of human adipose-derived mesenchymal stem cells in inflammatory stress-induced senescence features of osteoarthritic chondrocytes. Aging. 2016;8(8):1703–17.
49. Razani B, Lisanti MP. Two distinct caveolin-1 domains mediate the functional interaction of caveolin-1 with protein kinase A. Am J Physiol Cell Physiol. 2001;281(4):C1241–1250.
50. Wang P, Zhu F, Tong Z, Konstantopoulos K. Response of chondrocytes to shear stress: antagonistic effects of the binding partners toll-like receptor 4 and caveolin-1. FASEB J. 2011;25(10):3401–15.
51. Petit MM, Meulemans SM, Alen P, Ayoubi TA, Jansen E, Van de Ven WJ. The tumor suppressor scrib interacts with the zyxin-related protein LPP, which shuttles between cell adhesion sites and the nucleus. BMC Cell Biol. 2005;6(1):1.
52. Petit MM, Meulemans SM, Van de Ven WJ. The focal adhesion and nuclear targeting capacity of the LIM-containing lipoma-preferred partner (LPP) protein. J Biol Chem. 2003;278(4):2157–68.
53. Li B, Zhuang L, Reinhard M, Trueb B. The lipoma preferred partner LPP interacts with alpha-actinin. J Cell Sci. 2003;116(Pt 7):1359–66.
54. Wang H, Wu J, Ling R, Li F, Yang Q, He J, Lei X, Wu C, Zhang G, Zheng B, et al. Fibroblast-derived LPP as a biomarker for treatment response and therapeutic target in gastric cancer. Mol Ther Oncolytics. 2022;24:547–60.

Publisher's note